JOURNAL OF SOLID STATE CHEMISTRY 24, 209–218 (1978)

# A Series of Lead Tungsten Bronzes

THOMMY EKSTRÖM

*Department of Inorganic Chemistry, Arrhenius Laboratory, University of Stockholm, S-106 91 Stockholm, Sweden*

AND R. J. D. TILLEY

*School of Materials Science, University of Bradford, Bradford BD7 1DP, West Yorkshire, England*

Received July 20, 1977; in revised form October 3, 1977

The phases in samples of gross composition $Pb_xWO_3$ ($0.01 \leqslant x \leqslant 0.28$) heated at temperatures between 973 and 1373°K have been investigated. At all temperatures a nonstoichiometric tetragonal tungsten bronze phase forms for compositions $x > 0.18$. At temperatures up to 1273°K a series of orthorhombic intergrowth bronzes also forms, but these appear to be unstable at higher temperatures and were not found in the preparations made at 1373°K. Aspects of the crystal chemistry of these latter materials are discussed, including structure, crystal habit, valence of the Pb atoms in these phases, and the relation of the phases found here to other related intergrowth bronze phases.

## Introduction

Recently the crystal chemistry of ternary tungsten oxides has received increasing attention in view of the variety of different structure types which occur. This is particularly so in the composition region near to tungsten trioxide, $WO_3$, where crystallographic shear (*CS*) phases, a variety of oxide bronze phases, and pentagonal column (*PC*) structures have all been found to form (*1*). Because of this complexity, no satisfactory correlation has yet been found between the chemical nature of the ternary metal *M* and the resulting structure type, and a program of investigation has been undertaken to try to clarify the issues involved. As a part of this program we have started an investigation into the structure types formed in the Pb–W–O system near to $WO_3$ to complete studies on the related systems consisting of Ti (*2*), Zr (*3*, *4*) of the group IVA transition metals and Ge (*5*) and Sn (*6*) of the group IVB metals.

The only previous studies of the Pb–W–O system in the area of interest are by Bernoff and Conroy (*7*). These authors prepared a nonstoichiometric $Pb_xWO_3$ bronze of the tetragonal tungsten bronze (*TTB*) type in preparations made at 1423–1473°K, with a stoichiometry range varying from $Pb_{0.16}WO_3$ to $Pb_{0.35}WO_3$, but did not report a bronze phase in the interval $WO_3$ to $Pb_{0.16}WO_3$. The only other publication of note is that of Chang (*8*) who studied the $PbO–WO_3$ pseudobinary system, and who found that the compound nearest in composition to $WO_3$ was $PbWO_4$, with the scheelite structure.

The present paper reports on the results of a phase analysis of the $Pb_xWO_3$ system at temperatures between 973 and 1373°K. At 1373°K our results are in broad agreement with those of Bernoff and Conroy, but at lower



0022-4596/78/0242-0209$02.00/0

temperatures a series of $Pb_xWO_3$ bronzes has been found which appear to be structurally related to those occurring in the $Sn_xWO_3$ (*6*) and $K_xWO_3$ (*9*) systems. These findings are discussed in the light of the known crystal chemistry of other *M*–W–O ternary systems.

## Experimental

For some preparations the starting materials used were $H_2WO_4$ (Matheson, Coleman and Bell, p.a.) and Pb (Allied Chem. & Dye Co., p.a.). $WO_3$ was prepared by heating $H_2WO_4$ in air at about 1100°K and checked by X-ray powder diffraction. Appropriate amounts of Pb and $WO_3$ were thoroughly mixed and heated in sealed evacuated silica tubes for 7, 14, and 21 days at temperatures 973, 1073, and 1373°K. A series of samples was also heated at 1173°K for 7 and 60 days. These ampoules were as full as conveniently possible and were principally used to study equilibrium phases. Other samples were prepared from specpure grade $WO_3$ and Pb (Johnson Matthey Ltd.) and were heated for 7 days at 1173 or 1273°K. In these, the Pb metal was placed in the ampoule first and the $WO_3$ was contained in a small silica test tube within the ampoule, so that the reactants were physically separated by a vapor path of at least 3 cm. These were mainly used to give information on the mechanism of the reaction between Pb and $WO_3$. All samples were quickly removed from the furnace after heating, but no particular precautions were taken to quench them especially rapidly.

All the preparations were investigated by recording their X-ray powder patterns at room temperature with a Guiner–Hägg focusing camera using strictly monochromatic $CuK\alpha_1$ radiation and KCl ($a = 0.62923$ nm) as an internal standard. Some crystals were also examined by X-rays using Weissenberg techniques. In addition, all samples were studied optically, using a Zeiss Ultraphot microscope and selected samples were examined in a JEM 100B electron microscope operating at 100 kV and fitted with a goniometer stage and a JSM 35 scanning electron microscope.

## Results

The results obtained by all techniques were in good agreement with each other, and they have allowed us to make a preliminary analysis of the phases occurring in the Pb–W–O system near to $WO_3$. However, it should be noted that not all the phases identified may be true equilibrium phases and a more extensive phase analysis over wider ranges of preparation conditions will be needed to clarify this. In particular the composition ranges of the phases and their long term stability need to be carefully studied.

With this proviso in mind we can say that at 1373°K the results were in broad agreement with those of Bernoff and Conroy (*7*). The principal ternary oxide formed was of the *TTB* type which seems to exist together with $WO_3$ at this temperature. The lower limit of the homogeneity range of the former oxide was about $x = 0.18$ and the lattice parameters of the tetragonal cell at this composition were $a = 1.220 \pm 1$ nm and $c = 0.3781 \pm 2$ nm. The upper phase limits of this material have not been determined in this study which deals with the $Pb_xWO_3$ system at compositions close to $WO_3$, but the cell dimensions of the *TTB* phase of composition $Pb_{0.28}WO_3$ were $a = 1.222 \pm 1$ nm and $c = 0.3784 \pm 2$ nm, which showed that the lattice parameters vary only slightly with composition. However, we can report that in samples with high Pb contents within the *TTB* region annealing for extended times gave rise to a few unidentified very weak additional lines on the powder X-ray patterns. To ascertain that these lines were not associated with a superstructure within the *TTB* phase, a number of crystals from a sample of overall composition $Pb_{0.28}WO_3$ were examined by the Weissenberg technique. No indications of any multiplied axis were found and the additional lines might therefore arise from an extremely small amount of an addi-

tional phase, which we have not tried to identify.

At the lower temperatures investigated a series of previously unreported phases has been found. These formed in samples of overall composition lying between $Pb_{0.01}WO_3$ and $Pb_{0.18}WO_3$ although the composition range over which they occur alone, without coexisting with either $WO_3$ or the *TTB* bronze phase is much smaller, from approximately $Pb_{0.03}WO_3$ to $Pb_{0.05}WO_3$. We shall refer to these phases as orthorhombic bronzes or intergrowth bronzes for reasons which will be clear later.

The X-ray powder patterns of the orthorhombic bronzes were never sharp and well defined, even for those samples which were heated for 60 days. However, the reflections with indices $(0, 2k, l)$ referred to the $WO_3$-like subcell were fairly sharp and also the strongest in the patterns. The corresponding $d$-values for these lines did not vary much between samples of differing composition, indicating that the $b$- and $c$ axes do not vary greatly from one orthorhombic bronze structure to another. The approximate lengths of these axes was found to be $b \approx 0.734$ nm and $c \approx 0.389$ nm.

The experiments in which the Pb was physically separated from the $WO_3$ showed conclusively that all the $Pb_xWO_3$ bronze phases were formed via a vapor reaction. In general crystals of the ternary oxides grew near the entrance of the small test tube which contained the $WO_3$, and on the surface of the original $WO_3$ itself. The material at the bottom of this small test tube was usually unchanged or slightly reduced $WO_3$. The bronze phase formed depended on the amount of Pb in the outer tube. If this was such as to make the overall composition of the tube richer in lead than approximately $Pb_{0.13}WO_3$, they were long needle- or lath-shaped crystals which powder X-ray diffraction showed to be of the *TTB* type. When the overall composition of the sample was lower in Pb content, lying between $Pb_{0.01}WO_3$ and $Pb_{0.1}WO_3$ the ternary crystals formed had a characteristic platelike habit. X-ray diffraction confirmed that these had a structure differing from $WO_3$ or the *TTB* type and electron microscopy showed that they were intergrowth bronzes.

The same three crystal habits were also found in the other preparations. In this case though, only two sorts were usually present in a tube, indicating a closer approach to equilibrium conditions. These samples were studied by scanning electron microscopy as well as optical microscopy, and this technique was able to reveal clearly that the platelike crystals of the orthorhombic bronzes were almost always disordered so that they resembled a stack of cards. Thus they could readily be distinguished both from $WO_3$ which has a more cubic habit or the *TTB* phase, which is lathlike in habit. Figure 1a shows a typical scanning electron micrograph of crystals from a sample of overall composition $Pb_{0.05}WO_3$ showing plates and *TTB* crystals. Figure 1b shows a higher magnification image of a platelike crystal of the intergrowth bronze showing the stacking disorder typically found to be present. Weissenberg X-ray diffraction studies showed that these platelike crystals had a long axis of about 3.0 to 4.0 nm perpendicular to the surface of the plate and confirmed the disorder seen to be present by optical and scanning electron microscopy in this latter direction. The short axes had approximate dimensions $b = 0.78$ nm and $c = 0.38$ nm.

Using transmission electron microscopy these platelike crystals gave characteristic electron diffraction patterns in which the $WO_3$ subcell was clearly visible and in which one axis of the cell, designated as the $a$-axis here, was always subdivided by superlattice spots, as shown in Fig. 2a. We take this axis to be identical with the long axis found by X-ray diffraction and we assume that the other two shorter axes are normal to the $a$-axis, yielding an overall orthorhombic symmetry. It is convenient to classify these diffraction patterns and the phases giving rise to them by the same terminology used to describe the ortho-

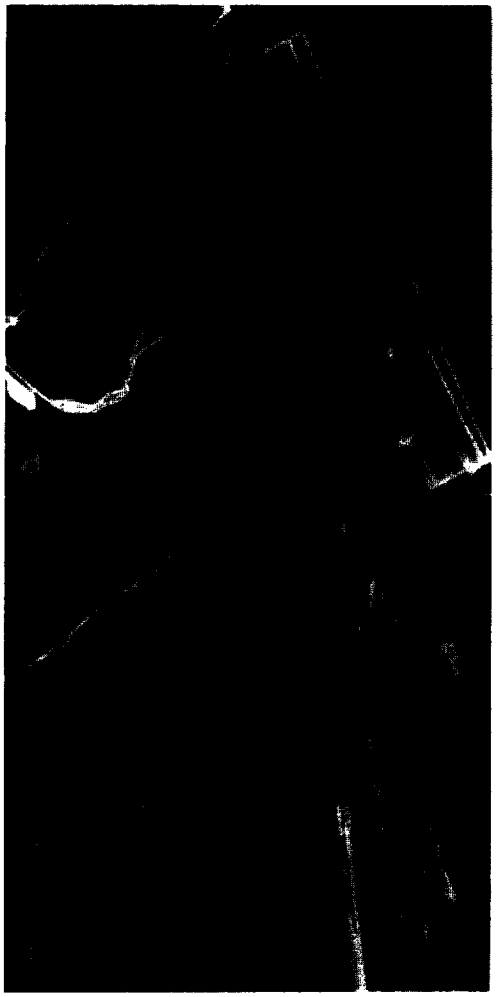

FIG. 1. (a) A scanning electron micrograph of part of a sample of gross composition $Pb_{0.05}WO_3$ to show that rodlike crystals are also present besides the platelike ones. These long thin lathlike crystals were almost always found in bundles and are the tetragonal tungsten bronze phase. Magnification on print 1500×. (b) A scanning electron micrograph of the edge of a platelike crystal to show the disordered stacking structure. Magnification on print 2500×. The plate was found in a sample of overall composition $Pb_{0.03}WO_3$ which consisted mainly of plates or fragments from plates. Generally the sheets that build the plates are from one to a couple of tens of nanometers in thickness.

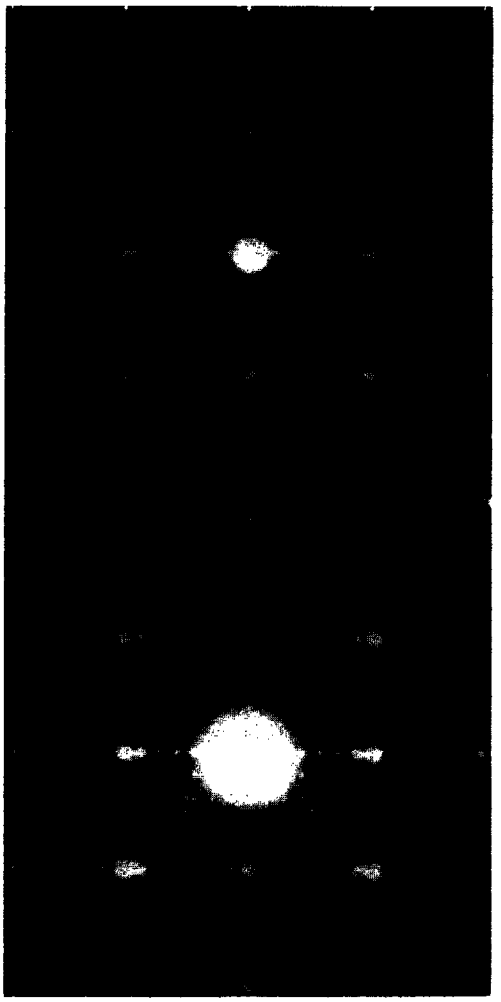

FIG. 2. Electron diffraction patterns from intergrowth bronzes found in samples of gross composition $Pb_{0.05}WO_3$, showing superlattice spots along (a) one $WO_3$ axis and (b) along two mutually perpendicular $WO_3$ axes. The square array of heavy spots are from the $WO_3$ subcell and show the relative dispositions of the superlattice reflections with respect to the $WO_3$ subcell.

rhombic $Sn_xWO_3$ bronzes (*6*). That is, to a reasonable approximation, along the *a* direction every *n*th spot is an intense $WO_3$ sublattice reflection, and the structure giving rise to this is called *n*-type. Thus Fig. 2a shows a 12-type material. In the present study the values of *n* found varied between 6 and 12 but other values outside this range may yet be found.

As a rule the number of superlattice spots increased as the nominal Pb content of the sample fell, so that 6-type patterns were seen most often in samples of overall compositions

between $Pb_{0.1}WO_3$ and $Pb_{0.13}WO_3$, while diffraction patterns showing 9 or more superlattice reflections were found in samples of overall composition between $Pb_{0.01}WO_3$ and $Pb_{0.05}WO_3$. However the samples examined were all inhomogeneous in this respect, and even samples heated for 60 days showed a variety of different superlattice types which was not noticeably narrower in range than those heated for just 7 days. In addition well-ordered electron diffraction patterns were not always found and frequently the rows of superlattice spots were also streaked, making it more difficult to count them precisely. More rarely a more complex arrangement of superlattice spots was seen on diffraction patterns, indicating a unit cell with at least two large dimensions. Such a diffraction pattern is shown in Fig. 2b. This type of pattern was found with equal frequency in both the shorter and longer time heated preparations.

Medium-resolution electron micrographs showed that the majority of crystal flakes were disordered. A typical example is shown in Fig. 3, where the dark lines mark planar boundaries or faults within the crystal. In order to obtain some structural information about these phases, high resolution electron micrographs were taken. An example of the images obtained when diffraction patterns of the type shown in Fig. 2a were used is shown in Fig. 4. Such micrographs revealed that the crystals consisted of slabs of $WO_3$, $n$ octahedra in width separated by planar faults which were usually dark and ill-defined in contrast. As in the case of the orthorhombic tin bronzes (*6*), this value of $n$ is approximately equal to the $n$-type recorded on the diffraction pattern. In all cases examined it was found that the slabs of $WO_3$-like structure were not displaced laterally with respect to one another on passing across a planar fault regardless of the number of octahedra, $n$, in the $WO_3$-like region.

When diffraction patterns of the general type shown in Fig. 2b were used for imaging a similar overall result was obtained. However, the contrast along the faults was now found to

FIG. 3. Medium-resolution electron micrograph showing the disordered structure of a typical crystal of an intergrowth bronze from a sample of overall composition $Pb_{0.05}WO_3$. Magnification on print 600 000×.

be markedly uneven. Figure 5 shows an example. It is readily seen that, although the image suggests that the crystal is not perfectly aligned in all regions, the contrast is similar to that shown in Fig. 4. This was taken to confirm that the contrast variations shown along the boundary regions were not spurious, and we tentatively identify this contrast variation with a partly ordered population of Pb atoms or ions in the fault planes. The contrast associated with Fig. 4 would then be related to a random distribution of Pb in the fault planes, or else a complete filling of each available site.

The only other structure types seen in the examples examined was either $WO_3$ or else slightly reduced $WO_3$ containing a small density of disordered {102} *CS* planes. As


FIG. 4. High-resolution electron micrograph of a typical crystal fragment of an intergrowth bronze showing the structure to be composed to $WO_3$-like lamellae separated by planar faults.

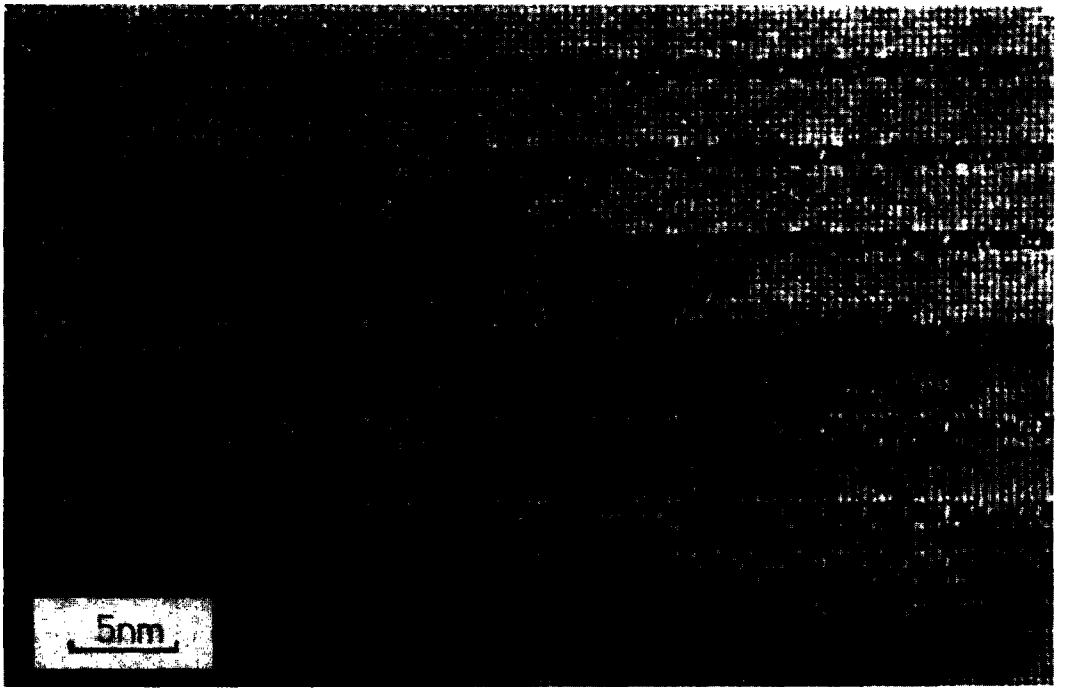


FIG. 5. High-resolution electron micrograph of a fragment of a crystal of an intergrowth bronze, suggesting that there is a partial ordering of Pb atoms or ions within the fault planes.

these structures have been illustrated in the past (*10–12*) they will not be shown here.

## Discussion

Our results for samples prepared at 1373°K are in reasonable agreement with those of Bernoff and Conroy (*7*) and show that at this temperature samples of gross composition $Pb_xWO_3$ result in the formation of a non-stoichiometric *TTB* structure and $WO_3$, which, under the experimental conditions employed in our studies, was sometimes slightly reduced. The most interesting result was the discovery of the orthorhombic bronze phases which form at somewhat lower temperatures and it is these results that we will discuss in most detail below.

### *The Structures of the Orthorhombic Bronzes*

The results show that the orthorhombic bronzes have a structure composed of sheets of $WO_3$-like material interspersed with fault planes parallel to ($h$00). In this respect they resemble the (00$l$) *CS* phases found in the $Nb_2O_5$–$WO_3$ oxides (*13*) and the orthorhombic bronzes reported in the Sn–$WO_3$ (*6*) and alkali metal–$WO_3$ systems (*9*). The actual structure of the fault planes themselves is of particular interest, and the results obtained go some way toward clarifying this. However, it is in general necessary to compare the image contrast observed on micrographs with that computed from electron diffraction theory before unequivocal assignments can be made, and so the following discussion should be regarded as qualitative rather than quantitative.

There are several possible structures which may be considered as models for the fault planes, (00$l$) *CS* planes, rows of double hexagonal tunnels as found in some alkali metal bronzes (*9*) and tin bronzes (*14*), rows of single hexagonal tunnels, or fault structures similar to those reported for the orthorhombic tin bronzes (*6*). These structures are shown in Fig. 6.

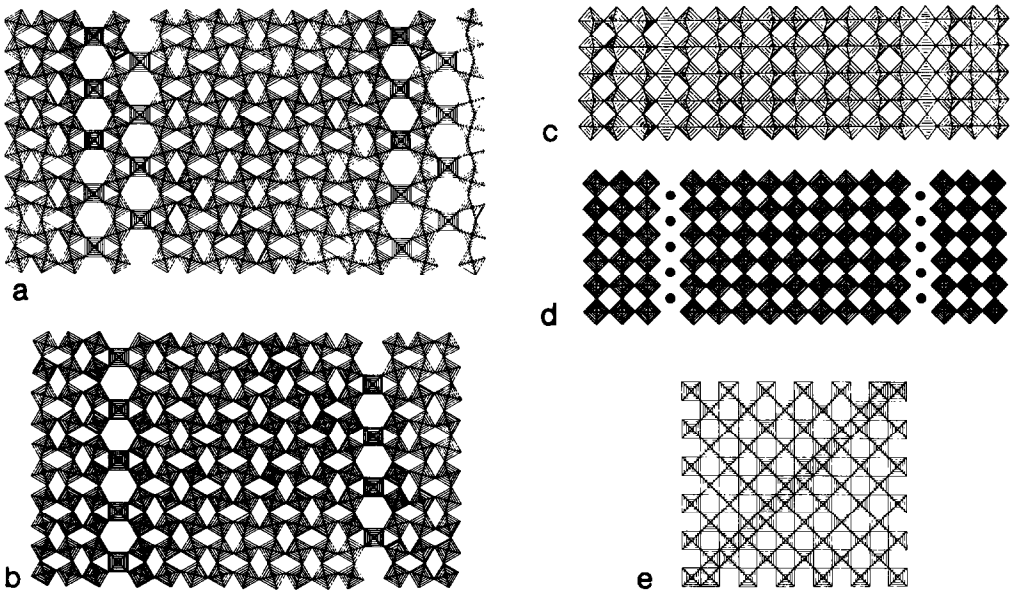


FIG. 6. The octahedral $WO_6$ frameworks of some structures in which $WO_3$-like lamellae are united along fault planes. (a) hexagonal intergrowth bronzes (*9*); (b) similar to (a) with single sheets of hexagonal tunnels, *a b* projection; (c) single sheets of hexagonal tunnels, *a c* projection; (d) orthorhombic tin tungsten bronzes (*6*); (e) (001) *CS* planes. In all these structures, only the $WO_6$ octahedra are shown except in (d) where the filled circles represent the likely positions of the tin atoms.

The experimental evidence allows some discrimination between these alternatives. For example we can note that in none of the high-resolution micrographs taken were the $WO_3$-like slabs ever found to be displaced laterally with respect to one another on passing across a planar fault, regardless of the number of octahedra in the $WO_3$-like region. This rules out the possibility that the faults are (00*l*) *CS* planes in the *ac* projection shown in Fig. 6e. In addition double rows of tunnels would be considerably wider than the fault width estimated from micrographs such as Figs. 4 and 5 which makes this model for the faults less likely to be the correct one. In a similar way, the contrast is not consistent with the *ab* projection of the *CS* planes perpendicular to that shown in Fig. 6 or with a similar projection of structures containing double rows of hexagonal tunnels. It is, however, possible that the planar faults might be single rows of hexagonal tunnels as shown in Fig. 6b and c. Such single rows of tunnels have already been observed in the alkali metal bronzes described by Hussain and Kihlborg (*9*). In this case the $WO_3$-like slabs will not be displaced from each other and if the tunnels are partly filled with Pb this may account for the ill-defined contrast observed. Another alternative is the structure shown in Fig. 6d which fits the contrast on the electron micrographs well enough. This suggests that the fault structures might be similar to those proposed in the $Sn_xWO_3$ system. This latter structure would also seem to be reasonable from other points of view. The lead species are likely to be in the $Pb^{2+}$ state as it is a well-known empirical rule that metal ions in the $M_xWO_3$ bronzes are in lower valence states (*15*, *16*). The assignment of a $Pb^{2+}$ state to the lead is also in agreement with Mössbauer data on the related Sn compounds, which showed only the presence of $Sn^{2+}$ in the crystals (*17*). It is known that $Pb^{2+}$ ions readily accept a square arrangement of oxygen atoms of the sort expected to be present in the fault planes shown in Fig. 6d, as similar coordination occurs in the scheelite $PbWO_4$ and more especially in tetragonal PbO. This model, though, has a severe drawback in that the stoichiometry departs appreciably from $Pb_xWO_3$.

From the present results it is impossible to say with any confidence which of the suggested structural models for the observed fault planes will be nearer the true situation. Further information on the structure and stoichiometry of these phases must therefore await careful single crystal X-ray analysis.

### *Ordering and Formation of the Orthorhombic Bronzes*

Regardless of the real structure of the fault planes in the orthorhombic bronzes, the evidence from micrographs and diffraction patterns such as Fig. 2b and 5 strongly suggests that a partial ordering of the $Pb^{2+}$ ions can take place. The most commonly observed ordering pattern seemed to be two positions occupied followed by three empty. This suggests that the Pb atoms or ions may well be linked in pairs in the structure.

It was significant that this ordering along the fault planes occurred over a variety of differing homologs, and the thickness of the $WO_3$-like lamellae does not seem to be important in this respect. In addition the number of fragments of crystals which showed ordering within the fault planes did not increase significantly when samples heated for 60 days were compared with those heated for only 1 week. By the same token, the variation in the widths of the $WO_3$-like slabs was no different in samples heated for short or long times, and all samples examined were very inhomogeneous in this respect. These aspects suggest that the structures formed in the early stages of reaction persist during annealing and are not readily converted to one another after formation.

The preparation methods indicate that these phases form by way of a vapor reaction. The slowest growth direction is normal to the plane of the crystals, that is, parallel to the *a* direction. One possible growth mechanism

which is able to account for the microstructures of these phases can be derived by considering the arrival of tungsten–oxygen and lead–oxygen species at the site of a nucleus of an orthorhombic crystal. Initially we can suppose that the tungsten–oxygen vapor species condense to build up a layer of $WO_3$, perhaps nucleated on other $WO_3$ crystals. The lead species arriving via the vapor will be large and may not readily fit into such a structure. These will be continually rejected from the $WO_3$ region and will build up on the surface until their concentration is sufficient to give a stable layer of Pb atoms or ions. This sheet will form the fault plane and will assimilate the lead into the structure. Repetition of the cycle leads to the growth of an orthorhombic bronze structure. Ordering of the lead within the fault plane will be possible, but whether it takes place will depend largely upon kinetic factors such as the rate of arrival of vapor species and the speed at which the crystal grows. However, once further layers of $WO_3$ are laid down, movement of the lead and subsequent ordering would be hindered and probably difficult. Variations in the width of the $WO_3$-like layers may also be accounted for by fluctuations in the rate of arrival of the various species. A disordered crystal in which the $WO_3$-like slabs are irregular in thickness will have to undergo a complex solid-state reaction to order perfectly. This is also likely to be a difficult process and explains why the crystals annealed for 60 days were not significantly better ordered than those heated for shorter times.

This mechanism of crystal growth satisfactorily accounts for most of the salient features of the microstructures of the orthorhombic bronze crystals. One feature which is not accounted for is the correlation between the ordering pattern of the lead species from one fault plane to another. Figure 5 shows that pairs of $Pb^{2+}$ ions often seem to occur at the same positions in neighboring fault planes, although the correlation is not perfect. As this ordering is enforced between sites 2–3 nm apart short range chemical bonding would not seem to be responsible. It is possible that elastic strain of the $WO_3$-like slabs by the $Pb^{2+}$ ions in one sheet is responsible, as such energy terms seem to be important in controlling the microstructures of *CS* planes in slightly reduced tungsten trioxide (*18*). This speculation cannot be verified until the real structures of the Pb-containing layers is known with certainty.

*Comparison with Related Phases*

These intergrowth bronzes show a marked similarity with those of Sn (*6*) and to those of K, Rb, Cs, and Tl (*9*) and Ba (*19*). In considering the Sn orthorhombic bronzes the similarities, as would be expected, are marked. The range of $n$ values for the Pb compounds, 6 to 12, closely parallels the Sn compounds, 5 to 12. The major difference would seem to be found in the crystals richer in foreign metal than $M_{0.1}WO_3$. In the case of Pb, a *TTB* phase alone forms, while in the case of Sn, two phases are found which are of the same family as the alkali metal *ITB* phases of Hussain and Kihlborg (*9*). This difference may well reflect the fact that Sn ions are more easily able to tolerate the change from a 2+ state to a 4+ state than Pb or may simply reflect the smaller size of the $Sn^{2+}$ ion.

A comparison between these phases and the alkali metal analogs is not possible until the real structure of the fault planes is ascertained. Nevertheless it is clear that one factor which all these phases have in common is that they are formed by $M^{n+}$ ions which have a large ionic radius. For such ions, intergrowth bronzes seem to form, but the exact details of the regions uniting the slabs of $WO_3$ seem to depend upon the particular ions involved. However, a comparison of the ionic radii of the ions known to form these intergrowth phases with those which do not form them allows one to conclude that size alone is not the only factor of importance. For example, $Na^{1+}$ is larger than $Sn^{2+}$ and yet no intergrowth phases have been reported in the Na–

W–O system. Similarly $Ag^{1+}$ and $Bi^{3+}$ have sizes which suggest that intergrowth bronzes could form, but once again, none have been reported in the literature. In the case of Ag, higher pressures may be needed in any synthesis.

At present no simple explanation of why some of these ions form intergrowth phases while other ions do not is available. In order to try to outline the formation conditions of these phases and related perovskite bronzes, studies have been initiated in a number of $M_xWO_3$ systems, including Sr, Ba, Sb, Bi, and Ag. The results of these studies will be reported in the future.

## Acknowledgments

R.J.D.T. is indebted to the Science Research Council for an equipment grant. T.E. is grateful to Prof. Arne Magnéli for the experimental facilities put to his disposal and also to the Swedish Natural Science Research Council for sponsoring a part of these studies.

## References

1. T. EKSTRÖM, *Chem. Commun. Univ. Stockholm*, No. 7, (1975).
2. T. EKSTRÖM AND R. J. D. TILLEY, *Mater. Res. Bull.* **9**, 705 (1974).
3. T. EKSTRÖM AND R. J. D. TILLEY, *Mater. Res. Bull.* **9**, 999 (1974).
4. T. EKSTRÖM AND R. J. D. TILLEY, *J. Solid State Chem.* **19**, 227 (1976).
5. T. EKSTRÖM, E. IGUCHI, AND R. J. D. TILLEY, *Acta Chem. Scand. A* **30**, 312 (1976) and unpublished results.
6. R. STEADMAN, R. J. D. TILLEY, AND I. J. MCCOLM, *J. Solid State Chem.* **4**, 199 (1972).
7. R. A. BERNOFF AND L. E. CONROY, *J. Amer. Chem. Soc.* **82**, 6261 (1960).
8. L. L. Y. CHANG, *J. Amer. Chem. Soc.* **54**, 357 (1971).
9. A. HUSSAIN AND L. KIHLBORG, *Acta Crystallogr. A* **32**, 551 (1976).
10. M. SUNDBERG AND R. J. D. TILLEY, *J. Solid State Chem.* **11**, 150 (1974).
11. S. IIJIMA, *J. Solid State Chem.* **14**, 52 (1975).
12. J. G. ALLPRESS, R. J. D. TILLEY, AND M. J. SIENKO, *J. Solid State Chem.* **3**, 440 (1971).
13. J. G. ALLPRESS, *J. Solid State Chem.* **4**, 173 (1972).
14. R. STEADMAN, *J. Chem. Soc. Dalton*, 1271 (1972).
15. M. PARMENTIER AND C. GLEITZER, *J. Solid State Chem.* **17**, 255 (1976).
16. A. B. SWANSON AND J. S. ANDERSON, *Mater. Res. Bull.* **3**, 149 (1968).
17. I. J. MCCOLM, R. STEADMAN, AND A. HOWE, *J. Solid State Chem.* **2**, 555 (1976).
18. E. IGUCHI AND R. J. D. TILLEY, *Phil. Trans. Roy. Soc., A* **286**, 55 (1977).
19. T. EKSTRÖM AND R. J. D. TILLEY, to be published.